13C.6 EVALUATING MICROPHYSICAL PARAMETERIZATION SCHEMES FOR USE IN HURRICANE ENVIRONMENTS

Robert Rogers[1], Michael Black[1], Shuyi Chen[2], and Robert Black[1]
[1]NOAA/AOML Hurricane Research Division, Miami, FL 33149
[2]Department of Meteorology and Physical Oceanography

1. INTRODUCTION

While there are many factors (e.g., vertical shear, upper oceanic temperature structure, and low- and mid-level environmental relative humidity) that determine a tropical cyclone's intensity and rainfall, these properties are ultimately dependent on the magnitude and distribution of the release of latent heat within the core of the storm. Despite the recognition of this importance, improving our understanding and forecasting of intensity and rainfall remains an elusive goal for the operational and research communities. High-resolution (grid length ≈ 1-2 km) numerical models have been used as a tool to investigate these processes. While convective parameterization is avoided using high resolution, the parameterization of microphysical processes such as hydrometeor production, conversion, and fallout, is still necessary at this resolution. The dependence of these microphysical processes on the rainwater, ice and graupel distributions thus assumes great importance in determining latent heating distributions and, ultimately, tropical cyclone intensity and rainfall.

2. METHODOLOGY

In this study high-resolution (1.67-km) MM5 simulations of Hurricanes Bonnie (Rogers et al. 2003) and Floyd (Tenerelli and Chen 2002) are compared with observations from nine different storms in order to evaluate the ability of the models to reproduce the statistics of the distributions of vertical motion, reflectivity, and hydrometeor mixing ratio seen in the data. The observations used in the intercomparisons are tail-mounted vertical incidence Doppler radar data (vertical motion and reflectivity), microphysics probe data (hydrometeor concentrations), and flight-level data (vertical motion at flight level).

The microphysical parameterization scheme used in the simulations is a modified version of the Tao-Simpson (Tao and Simpson 1993; Scott Braun, personal communication) cloud microphysics scheme for all four meshes. The Tao-Simpson scheme, which was modified from Lin et al. (1983), is a bulk three-class ice scheme that contains prognostic equations for cloud water (ice), rainwater (snow), and hail/graupel, and it allows for the generation of supercooled water. This scheme includes the processes of condensation/ evaporation, freezing/melting, sublimation/deposition, autoconversion (i.e., aggregation) of cloud water (ice, snow) to form rainwater (snow, hail/graupel), collection by rainwater (snow), and accretion.

* *Corresponding author address:* Robert Rogers, NOAA/AOML Hurricane Research Division, e-mail: Robert.Rogers@noaa.gov

3. RESULTS

Figure 1 shows a comparison of model output and observations using contoured frequency by altitude diagrams (CFADs; Yuter and Houze 1994). These diagrams essentially plot the variation of probability distribution functions with height. Figure 1 shows CFADs of

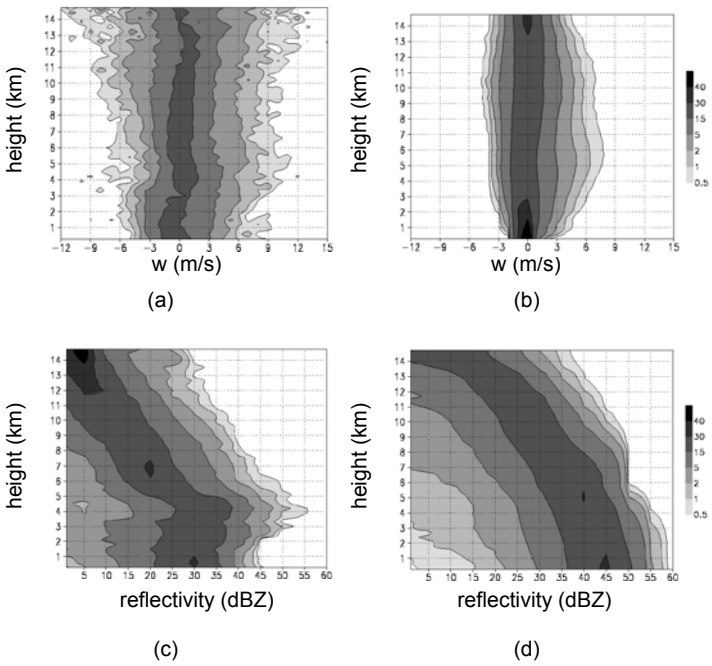

Figure 1. Contoured frequency by altitude diagrams (CFADs; shading, %) of Doppler-derived and simulated vertical motion for the eyewall region of (a) observed storms and (b) simulated storms and reflecitivity of (c) observed storms and (d) simulated storms.

vertical motion for the observations and simulations for the eyewall regions (Rogers et al. 2004) of all storms. As in Black et al. (1996), the majority of observed vertical motions (Fig. 1a) are weak ($|w| < 2$ m s^{-1}), but a small fraction (1-2%) of up- and downdrafts exceed 6 m s^{-1}. Values of observed vertical motion in the eyewall range from –6 to 9 m s^{-1} below the melting level. The distributions are fairly constant with height below the melting level, but they broaden with height above, indicating strong up- and downdrafts aloft for the extreme events (from –12 m s^{-1} to 12 m s^{-1}) at 13 km. The maximum frequency (*i.e.,* mode) of observed vertical motions is slightly negative in the lowest 2 km, but it becomes near zero or slightly positive above there. Above 9 km the mode of vertical motion is clearly upward, reflecting the loss of hydrometeors and reduction in water loading in the upper levels.

In contrast to the observations, the simulated vertical motion CFADs show a narrower distribution of vertical velocities. The majority of simulated up- and downdrafts are weak, similar to the observations, but values of the maxima are less than the observed values. Values in the lower troposphere range from –3 to 4 m s^{-1}. The range of upward motions increases with increasing height up to the melting level at 5-6 km, at which point the top 1% of points have upward motion of about 8 m s^{-1}. Above the melting level the maximum values decrease, but then there is another relative maximum at about 10 km. Above 10 km, the distribution narrows, in contrast to the observed distributions. The modal values in the eyewall are about zero in the lowest 2 km and become negative up until 8 km, above which it becomes slightly positive.

The observed eyewall reflectivity CFAD (Fig. 1c) is broadly distributed, with peak values around 45 dBZ in the lowest 2 km and values as high as 30 dBZ at 12 km for the top 1% of points. The distribution shows a slight decrease in reflectivity with height in the lowest 1-2 km, and then the values increase with height up to the melting level as warm rain processes cause an increase in hydrometeor mixing ratios. The distributions also show a maximum in reflectivity at the melting level, followed by a sharp drop-off above the melting level. The mode is 30 dBZ in the lower troposphere in the eyewall region.

In the simulations (Fig. 1d), the eyewall CFAD shows the high reflectivity bias commonly seen in simulations, as values approach 60 dBZ for the top 1% of points and the mode in the lowest 3 km is around 40-45 dBZ for the eyewall. At 6.5 km, the 45 dBZ value comprises nearly 15% of the points in the simulations, but it comprises only 0.7% of the points in the observations. The values of reflectivity in the top 20% of the distribution remain nearly constant or decrease slightly with height below the melting level. This slope is in contrast to the observations, which show an increase in height between about 2 km and the melting level. A significant difference between the CFADs of observed and simulated reflectivity is the fact that the decrease with height of reflectivity above 5 km is much smaller in the simulations than in the observations.

A scatter plot of flight-level vertical motion and probe measurements of hydrometeor mixing ratio for a portion of the flight track is compared with a scatter plot from an equivalent “flight-level” measurement from the model (Fig 2). The subsample of the flight track used was taken through a line of mixed convective and stratiform rain. As indicated by the linear regression lines fit to each distribution, there is virtually no relationship between observed vertical motion and mixing ratio at 9.9 km. The percent of variance explained by the regression line (r^2) is much less than the model, where values of cloud ice mixing ratio are less than 0.4 g kg^{-1} for updrafts weaker than 0.5 m s^{-1}, but increase to 0.6 g kg^{-1} for updrafts between 1.5 and 2 m s^{-1}.

A comparison similar to that done in Fig. 2a-b was performed for vertical motion and reflectivity from the radar dataset and the simulations of both Bonnie and Floyd (Fig. 2c-d). From the radar data (Fig. 2c), there is a fair amount of scatter between observed reflectivity

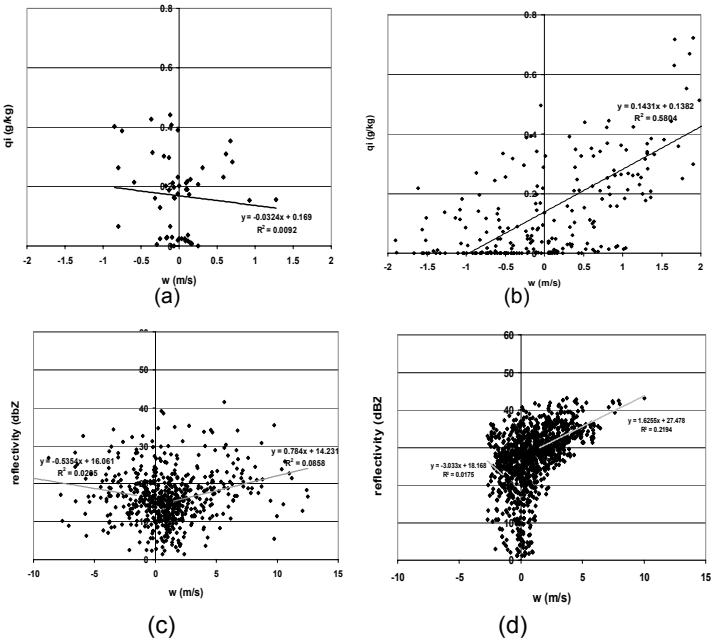

Figure 2. Scatter plots of flight-level vertical motion (m s^{-1}) and hydrometeor concentrations (g kg^{-1}) at 9.9 km for (a) observations and (b) simulation of Bonnie; and Doppler-derived vertical motion (m s^{-1}) and reflectivity (dBZ) for (c) all observed storms and (d) simulations of Bonnie and Floyd.

and vertical motion at 9.9 km. Two separate linear regression lines were calculated: one for vertical motions greater than 1.5 m s^{-1} and one for vertical motions less than -1.5 m s^{-1}. The slopes and variance explained of the regression lines for the updrafts and downdrafts are less than those for the simulations, indicative of a stronger relationship between vertical motion and reflectivity in the simulations.

4. FUTURE WORK

Future work will involve implementing improvements to the existing microphysical parameterization scheme based on the biases illustrated here and testing these improvements using the framework provided here. For example, one of the most apparent biases suggested by these results is that water loading is too prominent a factor in the simulations. This is supported by several differences between the simulations and the observations, e.g., the simulations consistently underdevelop the strongest vertical velocities and overdevelop the highest reflectivities; and the correlation between vertical motion and reflectivity and vertical motion and hydrometeor concentration is much stronger in the simulations than in the observations.

Other microphysical schemes, such as double-moment and spectral schemes, can be tested as well. These evaluation techniques can be used to compare not only parameterization schemes to observations, but also different parameterization schemes to each other. Furthermore, additional observational platforms, such as TRMM PR reflectivity fields and NASA EDOP vertical velocity and reflectivity fields from the NASA ER-2 aircraft, can be compared with the high-resolution simulations.

5. REFERENCES

References are available from the author by request.